



University of
Salford
MANCHESTER

A novel, soft, bending actuator for use in power assist and rehabilitation exoskeletons

Al-Fahaam, HSH, Davis, ST and Nefti-Meziani, S

<http://dx.doi.org/10.1109/IROS.2017.8202204>

Title	A novel, soft, bending actuator for use in power assist and rehabilitation exoskeletons
Authors	Al-Fahaam, HSH, Davis, ST and Nefti-Meziani, S
Type	Conference or Workshop Item
URL	This version is available at: http://usir.salford.ac.uk/id/eprint/47010/
Published Date	2017

USIR is a digital collection of the research output of the University of Salford. Where copyright permits, full text material held in the repository is made freely available online and can be read, downloaded and copied for non-commercial private study or research purposes. Please check the manuscript for any further copyright restrictions.

For more information, including our policy and submission procedure, please contact the Repository Team at: usir@salford.ac.uk.

A Novel, Soft, Bending Actuator for use in Power Assist and Rehabilitation Exoskeletons

Al-Fahaam, Hassanin¹; Davis, Steve² and Nefti-Meziani, Samia³

Abstract— This article presents the development of a fully soft, exoskeleton robot for power augmentation and rehabilitation of a human wrist joint. The system is powered by novel bending pneumatic muscles which have been combined with contractor pneumatic muscles to provide actuation for the glove. This research has assessed the behaviour of the new bending actuators and demonstrated them in a prototype wrist exoskeleton. An accompanying mathematical model of the force generated by the proposed extensor bending artificial muscles has been developed. The proposed wearable robot is capable of producing flexion-extension and abduction-adduction motions of the human wrist to generate rehabilitation motions. The exoskeleton is designed to fit any adult hand size without the need for any mechanical changes, meaning it can easily be swapped between users.

I. INTRODUCTION

Human upper-limb robotic devices can generally be split into two types [1]: prosthesis and orthosis. A prosthesis is an artificial body part such as a hand or leg that a disabled person can wear to replace a missing body part to help them in the activity of daily living. An orthosis is an orthopaedic device that can be utilized to straighten alignment or provide support to disabled individuals or to provide a functionality improvement for a limb which is still present but damaged in some way. In addition, orthosis devices are located outside the human body and provide a suitable external force to support the desired movement of the human limb. Traditional orthoses tend to be passive; however, the most recent development in the field have seen the introduction of wearable robot technology [2], [3]. Wearable robots have been extensively researched in the fields linked to rehabilitation devices, assistance robots, human force augmentation, impairment evaluation, and impedance exercises [4]. Power assistive and rehabilitation robots have increased in number particularly to assist physically weak elderly individuals and disabled people who have neurological damage, to improve their quality of life and independence. So as to provide the exoskeleton wearer with comfort and safety, the field of physical human-robot interaction has a considerable role to play in system design. This includes aspects such as the transmission of forces, actuator selection and the natural anatomical variation between people as well as the systems degrees of freedom,

dexterity, compliance and kinematics. A power assistive and/or rehabilitation exoskeleton must be; safe because it has a direct interaction with the patients or elderly individuals, lightweight to be a portable so that it can be used at home without any clinical assistance, and soft and small to be unobtrusive in independent daily usage. Many of these features exist in soft pneumatic artificial muscles and they have been used to build exoskeletons, and there are numerous examples of research based on these soft artificial muscles to construct force assist and/or rehabilitation wearable robots [5].

Human bodies, with their limbs joints flexibility, have the capability of performing numerous movements in a very effective and precise manner under different conditions in different environments with high flexibility. Inspired by the human body, researchers have presented many kinds of actuators [6], [7], [8].

In this paper, a soft wearable robot based on soft artificial muscles is developed. The major contributions of this research are a fully soft actuation system based on novel bending pneumatic muscles and contracting artificial muscles and a new mathematical model of the force generated by the proposed bending artificial muscles. The paper also describes the development and construction of a fully soft wrist exoskeleton to fit any adult hand without the need for any mechanical changes when it is swapped between users. The soft exoskeleton is capable of performing flexion-extension and abduction-adduction motions of the human wrist joint during rehabilitation exercises.

II. PNEUMATIC SOFT ARTIFICIAL MUSCLES

Pneumatic soft artificial muscles are driven by air pressure and are created from soft materials such as rubber tubes acting as a bladder and braided sleeves. They are inherently safe actuators for direct human interaction because of their light weight and lack of rigid parts. These features also make them suited to use in exoskeleton robots. The Pneumatic Artificial Muscle (PAM) [9], also called McKibben Muscle, is a tube-like actuator that is characterized by an increase or decrease in length when inflated or deflated [10]. The PAM is generally designed and constructed from a rubber or latex bladder tube which is encased by a braided sleeve and secured to rigid caps at both terminal ends. The PAMs transform applied pneumatic pressure into either a compressive or tensile force. These actuators have many advantages, for example, high power to weight ratios, the ability to be used as a direct drive, inherent safety, compliance and low cost. The main disadvantage of this type of muscles, it is has nonlinear behaviour. Because of this nonlinearity, it is difficult to modelled and control it.

¹ Hassanin Al-Fahaam is with the Department of Automation & Robotics, University of Salford, UK (Mobile: +44(0)744-055-3824; e-mails: h.s.h.al-fahaam@edu.salford.ac.uk & h.s.h.al-fahaam@ieee.org).

² Steve Davis is a Lecturer in Manufacturing, Automation & Robotics, University of Salford, UK (Phone: +44(0)161-295-3228; e-mail: s.t.davis@salford.ac.uk).

³ Samia Nefti-Meziani is a Professor of Artificial Intelligence and Robotics, University of Salford, UK, (Phone: +44(0)161-295-4540; e-mail: s.nefti-meziani@salford.ac.uk).

The proposed soft exoskeleton consists of both contracting artificial muscles and novel bending muscles. Contracting muscles have been widely studied and described in the literature. Their performance has been characterised and the basic mathematical modelling approach was based on the geometric characteristics of PAM. The models of [7], [8] have been widely used. Chou and Hannaford's model was based on static features of the soft actuator; they assumed that the muscle is cylindrical in shape, ignored the extensibility of the threads in the sleeve, ignored the friction force between the braided sleeve and the bladder and between the threads of the sleeve, and ignored rubber bladder forces. Others have advanced this model and the behaviour of contracting pneumatic muscles is well understood. For this reason the operation of contracting pneumatic muscles will not be described in depth in this paper; however, it is useful to describe the design and performance of the specific contractor muscles used in this research.

III. CONTRACTION ARTIFICIAL MUSCLES

The contractor muscles used in this research are constructed from a braided nylon sleeve, length 20cm and 10mm in diameter; an inner bladder formed from two layers of latex rubber tube 20cm length and 10mm diameter and two 3D printed caps ends, one with a closed terminal and the other with a hole through which compressed air can be supplied. Fig. 1 shows the proposed contracting muscle at different supplied pressures.

The characteristic relation between the supplied air pressure and the contraction amount is illustrated in Fig. 2. The contraction occurs when increasing the supplied pressure and this results in the creation of a contractile force. The maximum contraction ratio of the actuator used is approximately 30%. The force generated by the contracting muscle was determined experimentally, Fig. 3 shows these results as well as the theoretical force calculated using the mathematical model developed by [7].

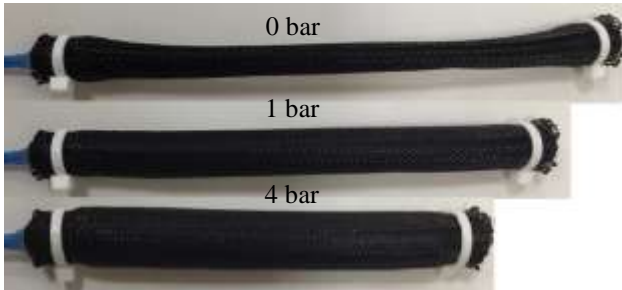


Figure 1. The contraction muscle with different pressures.

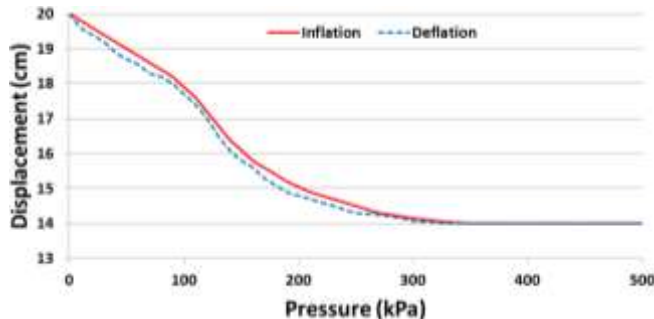


Figure 2. Measured muscle contraction with the applied pressure.

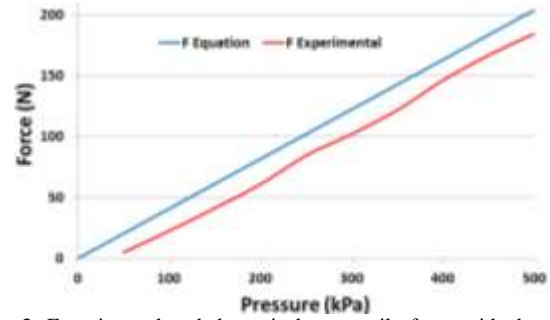


Figure 3. Experimental and theoretical contractile force with the applied pressure.

IV. BENDING ARTIFICIAL MUSCLE

The novel bending artificial muscle is developed using the same braided sleeve, bladder and 3D printed ends as in the contractor muscle. However, in this case, the sleeve length was double that of the bladder giving the muscles a resting diameter of 23mm. Due to the braid being longer than the bladder this means that the muscle will extend in length when the supplied pressure is increased, this type of muscle is known as an extensor. Fig. 4 illustrates the behaviour of the proposed extensor artificial muscle under different supplied pressures (without any load attached). It can be seen that the extensor artificial muscle expands as the supplied air pressure is increased. The maximum increase in the muscle length was measured experimentally to be 68%. This maximum increase in the actuator length is recorded at supplied air pressure 500kPa.

Fig. 5 shows the characteristic behaviour of the proposed extensor actuator in relation to the supplied pressure. During this operation, an axial extensile force is produced at the free end of the muscle. The bending artificial muscle is derived from the extending muscle by reinforcing one side of it using a fixed length thread with a 500N breaking strength and leaving the other side free. Fig. 6 shows the same bending muscle with different applied pressures.



Figure 4. The extensor muscle with different supplied pressures, where: L_0 is the muscle length at the rest, L_n is the muscle length under pressurization and ΔL is the amount of length increase.

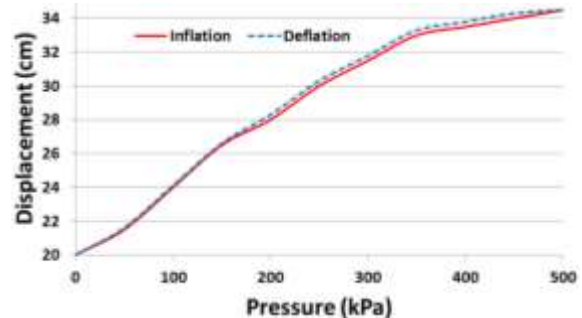


Figure 5. The length of the extensor muscle related to the supplied pressure.

When pressure is increased to the bending artificial muscle, the bending angle starts to increase in proportion with increasing pressure because it is forced by the thread to extend on the free side only.

The curving angle of the extensor bending muscle increases with increasing supply pressure and this relationship was investigated experimentally. The pressure inside the muscle was progressively increased and the angle of the remote terminal of the actuator with respect to its initial position was measured. Fig. 7 outlines the relationship between the provided pressure and the curve angle of the proposed bending actuator. It can be seen that the bend angle is proportional to the air pressure.

V. KINEMATIC ANALYSIS OF THE BENDING ACTUATOR

The general geometry of pneumatic artificial muscles (PAMs) is illustrated in Fig 8. The middle part of the PAM is completely cylindrical and the PAM has diameter D , length L , and θ is the angle between a single braid thread and the muscle's central axis. The braid is shaped from numerous individual strands of length b which encircle the muscle n times.

The difference between the extensor and the contractor type muscles is the braided sleeve is longer than the bladder in the extensor PAM. In other words, the braided sleeve must be compressed (θ increased) to make it fit with the bladder. The actuator initial state will have a braid angle greater than 54.7° (the minimum energy configuration [7]) when pressurized the braid angle will reduce in an attempt to achieve the minimum energy state and this will cause extension of the artificial muscle.



Figure 6. The bending artificial muscle with different pressures.

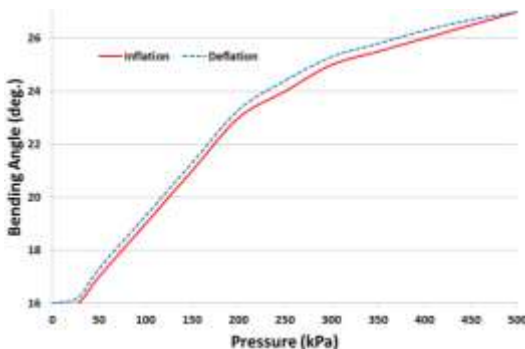


Figure 7. The bending angle of the proposed extensor bending muscle related to the supplied pressure.

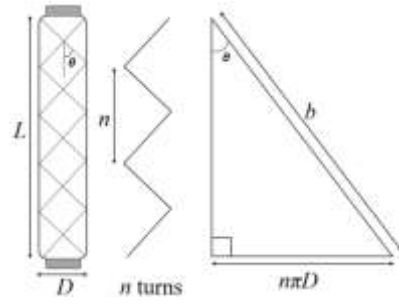


Figure 8. The general geometry of pneumatic artificial muscles.

As mentioned previously the bending actuator is derived from extensor actuator by reinforcing one side of the braided sleeve. In other words, that one side of the sleeve angle is always at its maximum value and cannot extend in length. When increasing the supply pressure of the bending actuator, the free side of the actuator, only, will increased in length.

Based on Fig. 8 the nominal length of the bending muscle will be:

$$L = b \cos \theta \quad (1)$$

and the actuator diameter:

$$D = \frac{b \sin \theta}{n\pi} \quad (2)$$

The analysis of the extensor bending artificial muscles based on the following assumptions: the muscle maintains a circular cross-section during bending, the braid is formed from inextensible threads, there are no friction forces between the rubber tube and the braid and between the braid threads and there are not elastic forces within the rubber tube.

Fig. 9 illustrates the curving artificial muscle geometry, where L_o is the actuator length on the fixed length side, L_n is the length of bending actuator on the free side, D_c is the bending actuator diameter, α is the curve angle of the actuator, r_o is the inner radius and r_n is the outer radius. The bending muscle length L_c will be the average length:

$$L_c = \frac{L_o + L_n}{2} \quad (3)$$

The muscle diameter relevant to the inner and outer radii is:

$$D_c = r_n - r_o \quad (4)$$

Using the equation for the length of an arc the length of the two sides of the bending muscle will be:

$$L_o = b \cos \theta_{max} = r_o \alpha \quad (5)$$

$$L_n = b \cos \theta = r_n \alpha \quad (6)$$

The inner radius r_o of the actuator curve can be determined by the maximum sleeve angle (θ_{max}), which is a constant for each bending muscle as a result of the fixed length side, and the outer radius of the actuator curve can be determined by the sleeve angle θ , which decreases as the actuator bends.

Unlike contraction PAMs the sleeve braid angle around the circumference of the curving actuator is not a fixed. Rather the sleeve angle will reduce around the circumference from θ on the outside edge of the curve (point A in Fig. 10) to θ_{max} at on the inward edge of the curve (point B in Fig. 10).

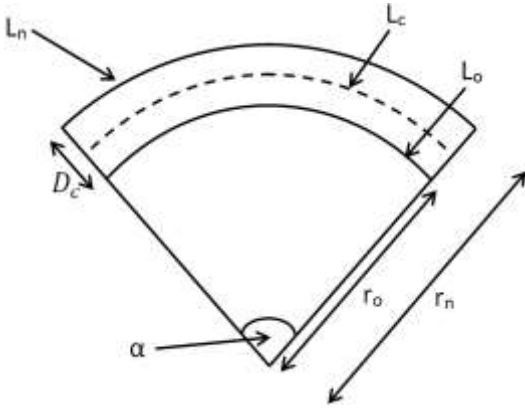


Figure 9. Curving artificial muscle geometry.

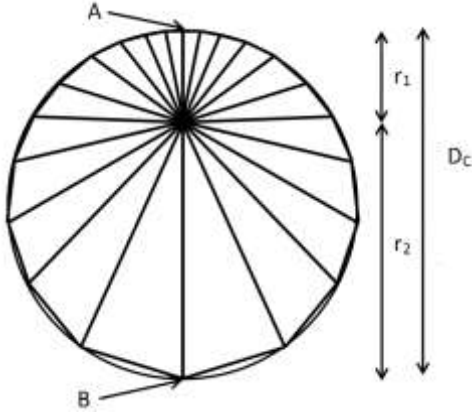


Figure 10. Radii inside bending actuator.

These sleeve angles will have an associated actuator diameter as illustrated in Fig. 10.

If it is assumed that the muscle cross is a perfect circle, then the overall diameter will be the sum of the radii on the outside of the bend r_1 and inside the bend r_2 as shown in Fig. 10. The bending muscle diameter can be found from (2) as the follows:

$$r_1 = \frac{D_1}{2} = \frac{b \sin \theta}{2n\pi} \quad (7)$$

$$r_2 = \frac{D_2}{2} = \frac{b \sin \theta_{max}}{2n\pi} \quad (8)$$

$$D_c = r_1 + r_2 \quad (9)$$

$$D_c = \frac{b \sin \theta + b \sin \theta_{max}}{2n\pi} \quad (10)$$

However, if the thickness (t_c) of the bladder and the sleeve is considered, the diameter equation will be:

$$D_c = \frac{b \sin \theta + b \sin \theta_{max}}{2n\pi} - 2t_c \quad (11)$$

Now it is possible to develop the kinematic equations of the proposed bending actuator by using the above information, these equations describe the bending angle α , and the central axis length of the actuator L_c as follows:

By combining (4) in (6), we will have:

$$L_n = (D_c + r_o)\alpha \quad (12)$$

Combining (5) and (6) in (12) produces the following equation:

$$L_n = \left(D_c + \frac{L_o}{\alpha}\right)\alpha = D_c \alpha + L_o = b \cos \theta \quad (13)$$

Based on (13) and (5) we can derive the bending angle as a function of braided angles θ and θ_{max} using the following equation:

$$\alpha = \frac{b \cos \theta - b \cos \theta_{max}}{D_c} \quad (14)$$

Furthermore, the actuator length can be determining by substituting (5) and (6) in (3):

$$L_c = \frac{b \cos \theta_{max} + b \cos \theta}{2} \quad (15)$$

VI. MODELLING THE OUTPUT FORCE OF THE BENDING ACTUATOR

The above section developed a kinematic analysis of the proposed bending actuator. However, if the actuator is to be utilized as a part of an application, it is vital that its output force behaviour is also characterised. This has been achieved using the theory of the conservation of energy as was presented by [7] for a contracting PAMs.

The input work W_{in} , which exists in the PAM is in the form of supplied air pressure, which acts on the inner surface of the artificial muscle, and leads to changes in muscle volume. This can be demonstrated by the following equation:

$$dW_{in} = \int_{S_i} (P' - P_o) dl_i \cdot d_{s_i} = (P' - P_o) \int_{S_i} dl_i \cdot d_{s_i} = P \cdot dV_c \quad (16)$$

Where P' is the interior absolute gaseous pressure, P_o is the environmental pressure (103.360 kPa at the time of testing), P is the relative differential gaseous pressure, S_i is the muscle total inner surface, dl_i is the internal surface displacement vector, d_{s_i} is the muscle area vector, and dV_c is the muscle volume change.

Depending on the formula of volume of the cylinder

$$V = \frac{\pi D_c^2 L}{4} \quad (17)$$

the bending muscle volume V_c will be:

$$V_c = \frac{\pi D_c^2 L_c}{4} \rightarrow V_c = \frac{1}{32 n^2 \pi} \left((b \cos \theta_{max} + b \cos \theta) \times (b \sin \theta + b \sin \theta_{max} - 4 n \pi t_c)^2 \right) \quad (18)$$

Where D_c is the bending actuator diameter from (11) and L_c is the central actuator length from (15).

The output work W_{out} done when the proposed curving actuator bends is associated with an increase in length of the muscle L_c as a result of the muscle volume changing. It can be expressed by the following equation:

$$dW_{out} = F \cdot dL_c \quad (19)$$

Fig. 11 illustrates the output force direction of the proposed bending actuator.

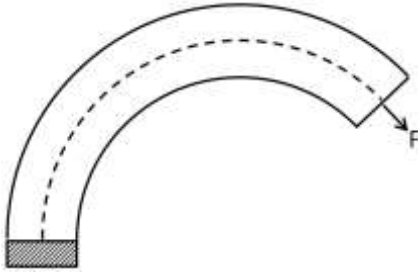


Figure 11. The output force direction of the bending actuator.

Based on the energy conservation theory, the change in input work is equal to the change in output work:

$$dW_{in} = dW_{out} \quad (20)$$

The proposed actuator output force can therefore be determined from (16) and (19) as follows:

$$F = P \frac{dV_c}{dL_c} \quad (21)$$

Differentiate the bending muscle volume and length with respect to θ gives:

$$\frac{dV_c}{d\theta} = \frac{1}{32n^2\pi} \times \quad (22)$$

$$(2b^2 \cos \theta (\cos \theta + \cos \theta_{max})(b(\sin \theta + \sin \theta_{max}) - 4n\pi t_c) - b \sin \theta (b(\sin \theta + \sin \theta_{max}) - 4n\pi t_c)^2)$$

and:

$$\frac{dL_c}{d\theta} = \frac{-b \sin \theta}{2} \quad (23)$$

The final mathematical model of the output force of the proposed extensor bending artificial muscle results from substituting (22) and (23) in (21) as follows:

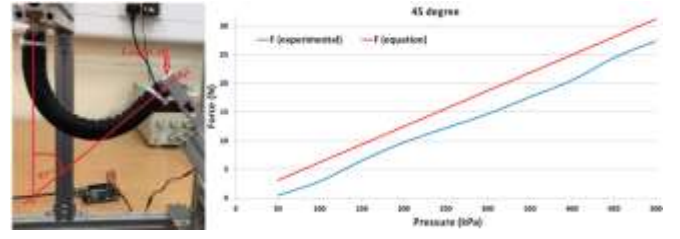
$$F = \frac{-2P}{32n^2\pi b \sin \theta} \times \quad (24)$$

$$(2b^2 \cos \theta (\cos \theta + \cos \theta_{max})(b(\sin \theta + \sin \theta_{max}) - 4n\pi t_c) - b \sin \theta (b(\sin \theta + \sin \theta_{max}) - 4n\pi t_c)^2)$$

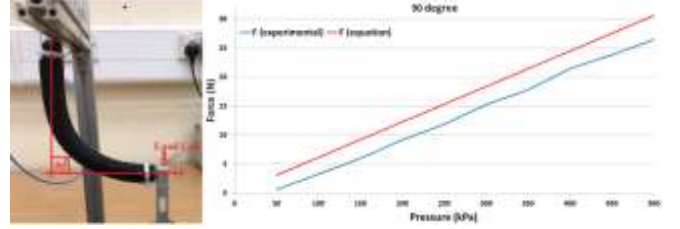
To validate this output force mathematical model of the bending muscles, we used the same muscle as in Fig 6.

The muscle is placed in three positions (bending angles) to validate that the force model is correct at any bending angle. Fig. 12 (a) shows the muscle at 45° bending angle and the graphs of the theoretical output force from the model at the same bending angle with the experimental results of the output force of the proposed actuator. It is obvious from the two curves; there is a small gap between the theoretical and the experimental output force (the free end of the muscle is reinforced to a load-cell to measure the experimental output force when changing the supplied pressure gradually) at this position. For validation of this model, we placed the same muscle at 90° bending angle as shown in Fig. 12 (b). In this case, we also measured the theoretical and experimental output force of the proposed muscle, and the match between the two curves was as expected. Another validation was performed at a bending angle of 135° as shown in Fig. 12 (c).

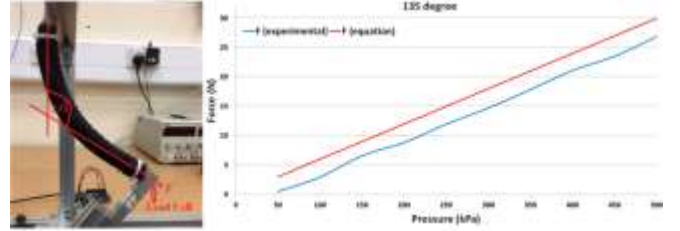
In the results of these three experiments, the average error across all three curved angles was calculated to be 3.7N. This represents an error of 12.05% of the maximum force generated by the proposed extensor bending artificial muscle.



(a) The actuator in 45°bending angle.



(b) The actuator in 90°bending angle.



(c) The actuator in 135°bending angle.

Figure 12. Three bending angles of the proposed actuator with their output force curves.

This error is expected as the mathematical model used is simplistic and does not take into consideration energy losses within the actuator.

VII. SOFT WRIST EXOSKELETON

Rehabilitation and physical therapy are successful methods of regaining the ability to control body motion for individuals with physical injuries, neurological damage and different kinds of disability. The most widely recognized are hand disability because the manual worker's hand is in direct contact with machines, and repeated motions at work cause neurological damage, which then produces a reduction of capability to control hand muscles.

There are a limited number of wrist rehabilitation movements such as flexion, extension, radial deviation (abduction) and ulnar deviation (adduction) [11]. The challenge is to accomplish all wrist motions using a single exoskeleton without any assistance from a rehabilitation therapist.

A lightweight, small, and simple to utilize wearable robot capable of performing wrist rehabilitation movements has been developed using a combination of contracting and bending pneumatic muscles as shown in Fig. 13. The air pressure supply to each actuator is controlled by MATRIX 3/3 solenoid valves which control the air flow by pulse width modulation.

Fig. 13 shows the prototype wrist force assist and rehabilitation wearable robot. The wrist flexion motion is generated by two (to increase power) extensor bending

actuators sewn onto the top face of a leather glove as shown in Fig. 14 (a). The extension movement is generated by a single contracting actuator located between the two bending muscles on the top of the glove as shown in Fig. 14 (b). Ulnar and radial deviation motions are produced by two contractor actuators placed along the sides of the leather glove which when activated cause the hand to move in either abduction or adduction as shown in Fig. 14 (c) and (d).

The overall weight of the proposed exoskeleton prototype is 0.15Kg. As the proposed exoskeleton is low weight and made from flexible materials, it is safe for direct human interaction and portable. It will also fit any adult hand size without the need for calibrate or mechanical changes making it suited to use in the home and without the need of a therapist.

The performance of this soft rehabilitation exoskeleton was assessed through some basic practical experiments. The pressure in the muscles was controlled in an open loop manner and it was shown that the system was capable of moving a user's wrist joint through flexion, extension, radial deviation and ulnar deviation motions.



Figure 13. The proposed wrist soft exoskeleton.



Figure 14. The rehabilitation movements of the proposed wrist soft exoskeleton; (a) Wrist flexion movement, (b) Wrist extension movement, (c) Wrist ulnar deviation movement (d) Wrist radial deviation movement.

VIII. CONCLUSION

This paper has described the initial phases of the design of a wearable force augmentation and/or rehabilitation exoskeleton for the human wrist which uses soft actuators. A novel bending pneumatic muscle has been proposed and its behaviour characterised experimentally. A kinematic analysis of the new actuator has been presented and a mathematical model of the actuators force output has been produced. The new bending pneumatic muscle has been combined with contracting muscles to form a soft glove which can fit any adult hand without the need for mechanical adjustment. Some initial rehabilitation motions have been demonstrated using the glove and future work will perform further analysis of the system when in operation, this will include monitoring EMG signals from a user's muscles to determine the amount of assistance the system is able to provide. Future work will also seek to improve the mathematical model of the new bending muscle by considering force losses in the bladder and braid during operation.

ACKNOWLEDGMENT

The authors would like to thank the ministry of higher education/Iraq, University of Basrah, computer-engineering department for providing scholarship support to the first author of this paper.

REFERENCES

- [1] R. Gopura, D. Bandara, K. Kiguchi, and G. Mann, "Developments in hardware systems of active upper-limb exoskeleton robots: A review," *Robotics and Autonomous Systems*, vol. 75, pp. 203-220, 2016.
- [2] I. Yamamoto, N. Inagawa, M. Matsui, K. Hachisuka, F. Wada, and A. Hachisuka, "Research and development of compact wrist rehabilitation robot system," *Bio-medical materials and engineering*, vol. 24, pp. 123-128, 2014.
- [3] S.-H. Chen, W.-M. Lien, W.-W. Wang, G.-D. Lee, L.-C. Hsu, K.-W. Lee, *et al.*, "Assistive Control System for Upper Limb Rehabilitation Robot," *IEEE Transactions on Neural Systems and Rehabilitation Engineering*, vol. 24, pp. 1199-1209, 2016.
- [4] P. Polygerinos, Z. Wang, K. C. Galloway, R. J. Wood, and C. J. Walsh, "Soft robotic glove for combined assistance and at-home rehabilitation," *Robotics and Autonomous Systems*, vol. 73, pp. 135-143, 2015.
- [5] H. Al-Fahaam, S. Davis, and S. Nefti-Meziani, "Power assistive and rehabilitation wearable robot based on pneumatic soft actuators," in *2016 21st International Conference on Methods and Models in Automation and Robotics (MMAR)*, 2016, pp. 472-477.
- [6] E. Kelasidi, G. Andrikopoulos, G. Nikolakopoulos, and S. Manesis, "A survey on pneumatic muscle actuators modeling," *Journal of Energy and Power Engineering*, vol. 6, p. 1442, 2012.
- [7] C.-P. Chou and B. Hannaford, "Measurement and modeling of McKibben pneumatic artificial muscles," *IEEE Transactions on robotics and automation*, vol. 12, pp. 90-102, 1996.
- [8] B. Tondu and P. Lopez, "Modeling and control of McKibben artificial muscle robot actuators," *IEEE control systems*, vol. 20, pp. 15-38, 2000.
- [9] X. Shen, "Nonlinear model-based control of pneumatic artificial muscle servo systems," *Control Engineering Practice*, vol. 18, pp. 311-317, 2010.
- [10] E. Kelasidi, G. Andrikopoulos, G. Nikolakopoulos, and S. Manesis, "A survey on pneumatic muscle actuators modeling," 2012, pp. 1442-1452.
- [11] H. Al-Fahaam, S. Davis, and S. Nefti-Meziani, "Wrist rehabilitation exoskeleton robot based on pneumatic soft actuators," in *International Conference for Students on Applied Engineering (ICSAE)*, 2016, pp. 491-496.